

(200)  
P. 270.

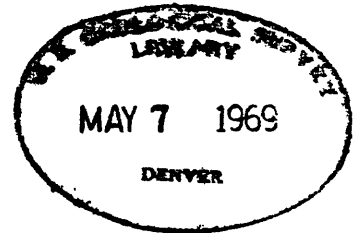
UNITED STATES  
DEPARTMENT OF THE INTERIOR  
GEOLOGICAL SURVEY

GEOLOGIC EVALUATION OF REMOTE SENSING DATA - SITE 157

ANZA-BORREGO DESERT, CALIFORNIA

by

Edward W. Wolfe



U. S. Geological Survey  
OPEN FILE REPORT **69-322**  
This report is preliminary and has  
not been edited or reviewed for  
conformity with Geological Survey  
standards or nomenclature.

CONTENTS

	Page
Introduction . . . . .	1
AN/AAS-5 Ultraviolet Scanner . . . . .	2
Black and White and False Color Photography.	3
Multiple-Filtered Color Infrared Photography	4
Multispectral Photography. . . . .	6
Thermal Infrared (8-14 Micron) Imagery . . .	7
Station 1. . . . .	8
Station 2. . . . .	10
Station 3. . . . .	14
Station 4. . . . .	17
Soil Moisture Problem. . . . .	18
Quality of Geologic Information. . . . .	22
Conclusions--Infrared Imagery. . . . .	23
Microwave Radiometer Data. . . . .	24
References . . . . .	26

## ILLUSTRATIONS

- Figure 1. Generalized geologic map of the Imperial Valley area, southern California (after Dibblee, 1954).
- Figure 2. High-altitude aerial photograph of site 157.
- Figure 3. AN/AAS-5 ultraviolet scan imagery, site 157, line 1.
- Figure 4. Black and white aerial photograph taken over anticline crest near center of line 1, site 157.
- Figure 5. Aero-Ektachrome Infrared (8443) aerial photograph taken over anticline crest near center of line 1, site 157.
- Figure 6. Kodachrome taken from 15,000 feet over axial portion of anticline near center of line 1, site 157.
- Figure 7. Kodachrome taken from a ridge top in the axial portion of the anticline near the center of line 1.
- Figure 8. Kodachrome showing pink sandstone and dark gray sandy mudstone exposed on southwest flank of anticline near center of line 1, site 157. Vallecito Mountains in background.
- Figure 9. False color photograph (Ektachrome Infrared 8443 + Wratten 15 filter) of same scene as figure 8.
- Figure 10. False color photograph (Ektachrome Infrared 8443 + Wratten 15 and CC30M filters) of same scene as figure 8.
- Figure 11. False color photograph (Ektachrome Infrared 8443 + Wratten 15 and CC30B filters) of same scene as figure 8.
- Figure 12. Transmission curves for Wratten 15, CC30M, and CC30B filters.
- Figure 13. Thermal infrared images of the eastern part of line 1, including station 1.
- Figure 14. Generalized geologic map of the Split Mountain-northwestern Fish Creek Mountains area (after unpublished geologic maps by Dibblee).
- Figure 15. Station 2. Cliff of barely consolidated pebbly sandstone overlain by bouldery gravel deposit. Bouldery colluvium discontinuously mantles sandstone outcrop. Truck stands on modern channel floor at base of cliff.

- Figure 16. Thermal infrared images of the southwestern part of line 2. Includes stations 2, 3, and 4.
- Figure 17. Thermal infrared image made shortly after midnight on May 24, 1968, northeast of the Salton Sea in the Salt Creek area. See figure 1 for location.
- Figure 18. Thermistor temperatures of surficial materials near San Andreas fault on northeast side of Salton Sea.
- Figure 19. Thermal infrared images of the western part of line 1.
- Figure 20. Microwave data, Mission 73, site 157.

GEOLOGIC EVALUATION OF REMOTE SENSING DATA - SITE 157,

ANZA-BORREGO DESERT, CALIFORNIA

by

Edward W. Wolfe

U.S. Geological Survey

INTRODUCTION

Remote sensing data were obtained at site 157 in May 1968 under Mission 73 of the NASA aircraft program. Those data as well as some previously obtained data are reported on herein. The site is located in an area of high temperatures and extreme aridity immediately west of the Imperial Valley, southern California.

Geologic studies by Dibblee (1954 and unpublished geologic maps) and Woodard (1963, unpublished doctoral dissertation) provide the geologic basis for evaluation of the imagery. Site 157 is partially surrounded by pre-Cenozoic crystalline rocks exposed in the Fish Creek, Vallecito, and Tierra Blanca Mountains (fig. 1). The study area itself is underlain by more than 20,000 feet of sedimentary strata of late Cenozoic age. The sedimentary rocks consist mainly of conglomerate, sandstone, and mudstone. A distinctive gypsum unit crops out in the northeast part of the area. Except for a few open folds shown in figure 2, the strata form a homocline dipping from approximately 10 to 30° to the southwest. Throughout much of the area the upturned strata have been eroded to badlands with relatively low relief.

## AN/AAS-5 ULTRAVIOLET SCANNER

Ultraviolet imagery was flown at an altitude of several thousand feet in the early afternoon of May 21, 1968. The segment along line 1, from Agua Caliente Springs to Lower Borrego Valley is shown in figure 3. The imagery produced by the scanner is of small scale--in this case approximately 1:180,000. Resolution is poor compared to the resolution of aerial photographs or Reconofax IV imagery from similar altitudes. Geologic features are poorly shown.

Dry stream channels floored with sandy alluvium appear bright in contrast to adjacent areas underlain by bedrock. In the western half of the image a northwest-trending grain parallels the strike of alternating sandstone and mudstone beds. In the eastern part of the image, the Fish Creek Mountains are dark. The very bright patch immediately west of the Fish Creek Mountains corresponds roughly with a bright area in aerial photographs and a dark anomaly on thermal infrared imagery. The anomaly covers the area of a gypsum crushing plant and may represent either gypsum dust in the air or reflection from a coating of gypsum dust at the plant and on the nearby valley floor. The extremely dark anomaly immediately to the south between Split Mountain and the Fish Creek Mountains occurs largely on a relatively flat alluviated valley floor.

Except for the bright sandy stream channels, geologic and topographic features are poorly displayed at best, and little geologic information supplementary to that apparent on aerial photographs was recognized.

## BLACK AND WHITE AND FALSE COLOR PHOTOGRAPHY

Aerial photographs (black and white 8401; Aero-Ektachrome Infrared 8443 plus Wratten 15 filter) were taken with RC-8 cameras over site 157 from an altitude of several thousand feet in the early afternoon of May 21, 1968. Photographs taken over the crest of the anticline located near the center of line 1 (fig. 2) were selected for comparison. The area shown in the photographs is underlain mainly by pink and light gray sandstones, greenish gray sandy mudstone, and red mudstone of the Palm Springs Formation. Kodachromes taken from 15,000 feet in the air (fig. 6) and on the ground from a low ridgetop near the anticline crest (fig. 7) illustrate the visual characteristics of the strata. Figure 6 in particular illustrates the high degree of discrimination of rock units that high quality color photography permits.

The 9-inch color infrared photograph (fig. 5) is overexposed at the center and underexposed in the corners due to vignetting. Exposure near the central part of the right edge is good; there contrasts among rock units are good in the black and white photograph (fig. 4) and excellent in the color infrared photograph (fig. 5). Discrimination can readily be made between dark gray sandy mudstone (dark tones in photographs) and the sandstone units (light tones). The two sandstone units are distinguished in places by color and outcrop style, but consistent distinction between the two sandstone types cannot be confidently made everywhere in these photographs. As a base for geologic field work, the color infrared photograph is better (granted exposure is correct

across the entire photograph) than the black and white because it shows clear color distinctions between features that may contrast indistinctly or not at all when portrayed in shades of gray.

#### MULTIPLE-FILTERED COLOR INFRARED PHOTOGRAPHY

Normally filtered color infrared photographs portray most rocks and soils in tones of bluish-green, and contrasts between rock units are often indistinct. Pease and Bowden (1968) have shown that color compensating filters can be used to enhance the photographic record of the longer wavelengths and to shift the color balance so as to eliminate the overwhelming blue-green cast of rock and soil in color infrared photographs. In order to test the suggestion, a 35 mm camera on a tripod was used to photograph a scene containing pink sandstones and dark gray sandy mudstones like those shown in figures 4 to 7. Both Kodachrome (fig. 8) and Ektachrome infrared (figs. 9-11) films were used. Color infrared film was exposed with Wratten 12, 15, 21, 22, 23A, 24, 26, and 29 filters by themselves and in combination with each of the following light balancing and color compensating filters:

80B  
82A  
CC10B  
CC30B  
CC50B  
CC10M  
CC30M  
CC50M

Potentially useful photography was obtained only with combinations involving Wratten 12, 15, and 21 filters. The other Wratten filters apparently cut off too much of the photographic spectrum to permit



useful display of rocks and soils. The 80B light balancing filter may have suppressed the upper part of the visible spectrum excessively, and the resulting photographs are overwhelmed by the red color that records infrared radiation. The 82A light balancing filter is similar in spectral character to the CC10B and produces similar false color photographs.

Photographs produced with the Wratten 15 (fig. 9), Wratten 15 plus CC30M (fig. 10) and Wratten 15 plus CC30B (fig. 11) filters were selected for illustration. The CC30M and CC30B are intermediate in density in the magenta series and blue series, respectively. Transmission curves for filters within a series (as CC10B, CC20B, CC30B, etc.) are similarly shaped and vary only in amplitude. Spectral character of visible light transmitted by the Wratten 15, CC30M, and CC30B filters is shown in figure 12.

Because of its haze-penetrating capability, the color infrared film (figs. 9-11) shows more detail than the Kodachrome (fig. 8) in the Vallecito Mountains--in the background of the photographs about five to ten miles from the camera. In the foreground areas, which range up to about a mile and a half in distance from the camera, the color infrared film (figs. 9-11) shows all of the color distinctions that appear in the Kodachrome (fig. 8). Some of these distinctions are enhanced when the Wratten 15 filter is used in combination with either the CC30M or CC30B filters (figs. 10 and 11). Color infrared film filtered with the proper color compensating filter in addition

to the normal Wratten filter may prove to be an extremely useful geologic tool because of the simplicity of the system, its haze penetration capability, and the high degree of color discrimination (albeit false color) among rocks and soils that it apparently offers.

#### MULTISPECTRAL PHOTOGRAPHY

Multispectral photography was flown along flight line 1 in late January 1968 by Stanford Research Institute. A 4-lens camera system provided by Cartwright Aerial Surveys was used with filters chosen to divide the visible and photographic infrared portions of the spectrum into 4 broad bands. Each band was recorded on 70 mm black and white film so that every scene photographed from the air was recorded by 4 black and white photographs. Sets of 4 positive transparencies representing several scenes along line 1 were made into lantern slides, and sets of 4 slides were projected simultaneously onto a screen using a battery of 4 projectors at the School of Forestry, University of California (Berkeley). Various combinations of colored filters, plus neutral density filters to modify the brightness of each record, were used to create false color composite images from the 4 simultaneously projected images in the hope that enhancement of significant geologic features would result. Good registry of the 4 images was not achieved, and none of the experimental film-filter combinations provided more geologic information or more contrast between geologic units than was already available in the black and white records of the red and near infrared portions of the spectrum. It seems likely that the 4 recorded

bands were too broad to permit discovery and utilization of differences in spectral character among the rock units. The multispectral technique will probably be most successful for distinguishing local lithologic units when filter selection is based on prior field measurement of spectra.

#### THERMAL INFRARED (8-14 MICRON) IMAGERY

Thermal infrared (8-14 micron) imagery was obtained with the Reconofax IV scanner from an altitude of several thousand feet. Flights were made in the early afternoon of May 21, before sunset on May 22, before and after sunset on May 23, and before and after sunrise on May 24. The pre-sunset imagery of May 23 closely duplicates that of May 22; the May 22 imagery is not considered further in this report.

RS-7 imagery (classified) obtained in September 1967 (Mission 56) from a higher altitude served as a basis for selection of ground monitoring sites during Mission 73. Ground monitoring, including continuous measurement of air temperatures and near-surface temperatures of surficial materials, was undertaken by R. Moxham and G. Greene of the U.S. Geological Survey. Near-surface temperatures of surficial materials were measured by thermistors inserted in cracks in rock or pushed into unconsolidated materials just far enough to bury the probes, discs a few millimeters in diameter. Measurements of specific gravity and moisture content of surficial materials were made by Wolfe. Specific gravity was measured in the field. Moisture content was determined after heating field-weighed samples for 24 hours at 65°C.

Latin American observers as well as USGS, NASA, and University of California personnel generously assisted in gathering additional data during the mission.

Continuously recorded near-surface temperature data were collected (1) on gypsum outcrop and a small alluvial fan at the north end of Split Mountain, (2) on alluvial deposits of two different ages and on sandstone bedrock in Vallecito Wash, (3) on the alluvial fan at the mouth of Indian Gorge and on the adjacent alluvial deposits at its margin, and (4) on granitic bedrock and alluvium in Indian Valley. These areas are denoted respectively as stations 1, 2, 3, and 4 in figure 2.

#### Station 1

Station 1 was established at the head of a small dissected alluvial fan in contact with Fish Creek Gypsum (figs. 13, 14). The fan consists of granitic cobbles and sand and gravel. The granitic cobbles form a discontinuous pavement over most of the fan surface. The broad outcrop of gypsum immediately southwest of the fan consists at the surface of gypsum powder overlain by a thin ( $\frac{1}{4}$ - to  $\frac{1}{2}$ -inch) porous gypsiferous crust. A deep narrow canyon dissecting the gypsum outcrop is floored by dense fresh gypsum. Specific gravity of the weathered porous gypsum was less than 1.0, of the fresh dense gypsum 2.2, and of the alluvial fan material (excluding cobbles) 1.6 (inclusion of cobbles would probably give a specific gravity value well above 2.0). Moisture contents were low--about 2 percent for weathered gypsum and about 1 percent for alluvial fan material (excluding cobbles).

The weathered gypsum is strikingly dark (low radiance) in the pre-sunset and post-sunset images (figs. 13a, b), and both the alluvial fan and the fresh dense gypsum on the canyon floor are bright (high radiance). Near-surface temperatures of the weathered gypsum in the near-sunset flights were 4°C. below those of the alluvial fan.

In the early morning images (figs. 13c, d) the weathered gypsum is still darker (less radiant) than the alluvial fan and the fresh dense gypsum of the canyon floor. The gypsum outcrop is less well defined, however, in the early morning images than in the early evening images, and near-surface temperature differences between the weathered gypsum and the alluvial fan were smaller (3°C. at the time of the pre-sunset image and less than 2°C. at the time of the post-sunset image) than in the near-sunset hours.

In the midday image (fig. 13e) the gypsum and the alluvial fan are indistinctly portrayed in similar shades of gray. Near-surface temperature data obtained 2 days after the daytime flight suggest that gypsum and alluvial fan temperatures are similar at midday.

The gypsum map pattern (fig. 14) at station 1 as well as elsewhere on the eastern flank of Split Mountain and at the northern end of the Fish Creek Mountains is closely reproduced in aerial photographs (e.g., fig. 2) as well as in thermal infrared images (particularly figs. 13a, b). Extensive gypsum outcrops are extremely dark (low radiance) in figures 13a and b and are bright (high radiance) only in the quarry, where the weathered porous gypsum has been removed

and fresh dense gypsum is exposed. The gypsum is bright (high reflectivity) in the aerial photograph. A similar relation occurs in the Temblor Range of southern California, where shale units that are dark in night-time imagery are bright in aerial photographs (Wolfe, 1968, p. 14).

The most obvious correlation between 8 to 14 micron radiance and physical properties is the correlation with specific gravity. In the early evening and early morning hours, weathered gypsum (low specific gravity) shows low radiance, and fresh gypsum and the alluvial fan as well as adjacent conglomerates of the Split Mountain Formation (all high specific gravity) show high radiance. Materials with low specific gravity have high porosity. Hence they have low thermal conductivity and their surfaces respond relatively rapidly to changes in ambient temperature. In addition the high reflectivity of the gypsum surface material may contribute insofar as it retards daytime absorption of solar radiation.

A prominent dark anomaly in the infrared images occurs on the alluviated valley floor beside the gypsum quarry. It coincides with an anomalously bright patch on aerial photographs that represents a coating of gypsum dust from the quarrying and crushing operation.

## Station 2

Station 2 was located in Vallecito Wash (fig. 2) at the base of a steep northeast-facing cliff about 100 feet high. The cliff, as well as the nearby hills west of Vallecito Wash, is underlain in part by

southwest-dipping pebbly sandstone of late Cenozoic age. The sandstone is very weakly consolidated, clean, and friable. Its specific gravity, measured in the field, is 1.7. A deposit of sandy gravel with abundant granitic and metamorphic cobbles and boulders caps most of the hills immediately west of Vallecito Wash including the cliff at station 2. The deposit forms a continuous upland sheet immediately west of the line of hills. Bouldery colluvium derived from the gravel deposit discontinuously mantles the hillsides including the station 2 cliff (fig. 15).

The broad alluviated surface of Vallecito Wash is about half a mile wide northeast of the station 2 cliff. Immediately at the base of the cliff about 4 feet lower than the adjacent alluviated surface is the flat alluviated floor of a modern channel about 125 feet wide. The surfaces of both the older alluvium and the modern channel floor are underlain by unconsolidated sand ranging in size from very fine-grained sand to granules. Specific gravity of the alluvial sand ranges from 1.4 to 1.8 and averages 1.6.

Moisture content near the surface in both the sandstone and the alluvial sand was less than 1 percent. At the time of the mission, visible interstitial moisture occurred below a depth of 6 to 12 inches in the modern alluvium but was not found at a depth of a foot in the older alluvium. The moisture may represent a residuum that was derived from runoff of the previous winter. It may have been restrained from draining downward by surface tension and protected from evaporation by the overlying dry sand.

The cliff face is more radiant than the alluvial deposits in both the early evening and early morning images (figs. 16a, b, c, d). Near-surface temperatures in the sandstone of the cliff were 0-0.5°C. warmer than those of the alluvium at the time of the pre-sunset flight, 1-2.5°C. warmer at the time of the post-sunset flight, and 3-4°C. warmer during the early morning flights. At the time of the midday flight, the sandstone outcrop was 12.5-18°C. cooler in near-surface temperature than the alluvial deposits. The cliff is less radiant in the midday image (fig. 16e) than the alluvium and was probably in partial shadow. Interestingly, a radiometer pointed at the sandstone outcrop in the cliff face recorded radiant temperatures as much as 11°C. below the night-time near-surface temperatures and as much as 5°C. above the daytime near-surface temperatures. Either steep temperature gradients occur just below the sandstone surface or the spots selected for temperature measurement were not representative. ✓

Moisture and specific gravity measurements as well as field observations of texture show the high degree of similarity between sandstone outcrop and alluvial deposits. The sandstone differs by being slightly more indurated, tectonically tilted, and intricately dissected.

Field observation and comparison of the imagery with the aerial photograph (fig. 2) show that in the eastern half of figures 16a, b, c, d the areas of high early evening and early morning radiance correspond with intricately dissected surfaces in which steep gullied slopes (typically 30° slopes) abound, and the areas of low radiance



correspond with relatively smooth surfaces characterized by low slope angles (typically less than  $10^\circ$ ). Intermediate slopes are scarce. The less radiant surfaces occur on uplands as well as in the low valley bottoms and include ridge crests near station 2. In and west of Vallecito Wash, surfaces of high early evening and early morning radiance are underlain by sandstone, bouldery gravel, and bouldery colluvium; surfaces of low radiance are underlain by alluvial sand and bouldery gravel.

Absence of significant differences in texture, specific gravity, and moisture content between alluvial sand and sandstone outcrop cast doubt on the hypothesis that differences in thermal properties are responsible for the greater night-time radiance of the sandstone outcrop. The consistent low radiance of the gently sloping surfaces, whether they be relatively high or low topographically, militates against hypotheses calling on local atmospheric anomalies (e.g., stagnation of cold air produced by night-time density stratification). Furthermore, air temperature measurements in the modern wash and on the slightly higher older alluviated surface showed no development of air stratification within 4 feet of the ground.

High early evening and early morning radiance is apparently related to the occurrence of steeply sloping surfaces (or scarcity of nearly horizontal surfaces) regardless of lithologic differences and similarities in the underlying materials. Steeply sloping surfaces "look at" a greater thickness of atmosphere and a smaller segment of cold sky than do nearly horizontal surfaces. Consequently steep

slopes may receive more night-time radiation from the atmosphere and from other ground surfaces and hence suffer a smaller net radiative loss than do horizontal surfaces.

### Station 3

Station 3 was located at the north edge of the alluvial fan formed where Indian Gorge debouches into the valley of Vallecito Wash (fig. 2). Scattered granitic cobbles occur on the lower part of the fan and become larger and more abundant toward its apex. Near station 3, both the fan surface and the adjacent valley floor are underlain by similar unconsolidated pebbly sand. The sharp north boundary of the fan does not represent an abrupt lithologic change but coincides with a small wash that follows the fan margin. The steep mountain front, 50 feet west of station 3, is underlain by pre-Tertiary granitic rocks.

The northern half of the fan is less radiant in the near-sunset and near-sunrise imagery (figs. 16a, b, c, d) than the valley floor against which it impinges; it is also less radiant than the southern half of the fan. The granitic rocks of the nearby mountain front are more radiant than either the fan or the alluviated valley floor. In the midday imagery (fig. 16e), the northern half of the fan is again less radiant than either the southern half or the immediately adjacent alluviated valley floor.

Near-surface temperatures measured during the near-sunset and near-sunrise flights show that a granitic boulder near the mountain

front was 2 to 4°C. warmer than the northernmost part of the fan; the northernmost part of the fan in turn was 1 to 2°C. warmer than the adjacent part of the alluviated valley floor. The near-surface temperatures of the fan and the valley floor correlate inversely with the radiance recorded in the imagery.

Near-surface temperatures were not recorded during the midday flight. On subsequent days, however, at the same time as the midday flight, near-surface temperatures near the north edge of the fan were within 1°C. of temperatures measured on a granitic boulder at the mountain front; near-surface temperatures of the alluvial deposits just north of the fan were 4 to 6°C. above those of the fan. Correlation between midday radiance (fig. 16e) and subsequently measured near-surface temperatures is poor. Radiance of the northernmost part of the fan is similar to that of the adjacent alluvial plain, and the mountain front is much less radiant than either. The near-surface temperature measurement points may not have been representative of the larger features that are resolved in the imagery.

The differing diurnal radiance patterns shown by the mountain front and the adjacent alluvial deposits (fan and valley floor) are explainable in terms of differing thermal inertia. The granitic rocks have greater conductivity, greater thermal inertia, and they show less response to external temperature change than do the unconsolidated alluvial deposits. Consequently the granitic rocks are relatively cool at midday. In addition, the granitic mountains are less reflective to solar radiation (fig. 2) and are dominated by steep slopes. Both of

these factors may contribute to the high early evening and early morning radiance of the granitic rocks.

The north half of the fan, however, is not texturally distinct from either the adjacent deposits of the valley floor or from the southern half of the fan. Nor is its relatively low radiance during both day and night the effect that one would expect a difference in thermal properties to produce. The aerial photograph (fig. 2) shows that the north half of the fan is more reflective (brighter) than either the southern half or the nearby alluvial deposits of the valley floor. The high reflectivity is related to the abundance of modern distributary channels on the northern half of the fan. Vegetation, both dead and alive, is less abundant on the active northern half of the fan, where the anastomosing distributaries have washed the fan surface relatively clean, than it is on either the adjacent valley floor or the southern half of the fan. Reflectivity is related to the proportion of clean light-colored sand at the surface and inversely related to the proportion of vegetation and dead vegetative matter. The more reflective materials (e.g., north half of the fan) may be less radiant either because of lower 8 to 14 micron emissivity (relative emissivities are unknown) or because of less absorption (greater reflection) of solar radiation during the daytime or both. A similar relation exists elsewhere in the study area between the clean white sand of the modern alluvial channels and the older, slightly darker alluvial deposits, whose surfaces contain a slightly greater concentration of vegetative debris.

#### Station 4

Station 4 was located approximately 2 miles upstream from the Indian Gorge fan (fig. 2). Indian Valley is about half a mile wide at this point and is bordered by steep slopes of granite that rise several hundred feet above the valley floor. The station was established at the south side of a granitic knob that rises approximately 80 to 200 feet above the valley floor and is surrounded by alluvium. The alluviated valley floor at station 4 is nearly flat in cross-section but slopes downstream (east) about 280 feet per mile. The alluvium consists of unconsolidated granitic debris ranging from very fine-grained sand to granules. Specific gravity of the alluvial sand was 1.6, and moisture was 0.2 percent. The granite is relatively fresh, and its specific gravity is probably close to 2.6. Moisture content of the granite is presumed negligible.

In the evening and early morning imagery (figs. 16a, b, c, d) the alluvium is dark (low radiance), and the granite is bright (high radiance). Near-surface temperatures were approximately 3°C. higher for the granite during the near-sunset flights and about 1°C. higher during the pre-sunrise flight. No data were collected during the post-sunrise flight. In the midday imagery (fig. 16e) the granite is less radiant than the alluvium. Midday near-surface temperatures measured on the day following the midday flight were 5°C. higher in the alluvium than in the granite.

Differences in thermal properties related to differing specific gravity--hence different porosity--explain most simply the diurnal radiance patterns illustrated at station 4. The granite is more dense

(less porous). As a consequence, its conductivity is greater than that of the alluvium, and its surface responds less readily to external temperature change. Hence the granite appears relatively warm at night and cool at midday. Steepness of slopes and low reflectivity may also contribute to the relatively great evening and morning radiance of the granite.

#### Soil Moisture Problem

A notable feature of the night-time infrared imagery flown on September 6, 1967 (Mission 56) was the distinctively low radiance of the shallow modern channels in the dry washes. Between August 15 and September 4, 1967, approximately 1 to 2 inches of rainfall was recorded at stations near site 157 (e.g., Ocotillo Wells, Borrego Desert Park, Coyote Wells). No field observations were made when the imagery was flown. It is unknown whether the channel floors were significantly more moist on the night of September 7 than the broad alluviated surfaces that they dissect. The suggestion that "cold" anomalies are directly related to soil moisture resulting from earlier rains is difficult to refute. Other workers (Wallace and Moxham, 1966; Sabins, 1967, p. 749) have suggested the possibility that some "cold" anomalies of this type may represent high soil moisture. On the other hand, Wolfe (1968, p. 20-25) found evidence suggesting that some "cold" anomalies at the base of the Temblor Range, California, might be related to night-time entrapment of cold air in poorly drained, topographically low areas rather than to the occurrence of soil moisture. In addition, evidence summarized later suggests that the effect of high soil moisture is to create a "warm" night-time anomaly rather than a "cold" one.

In order to test the idea that cold dense air draining through the modern channels created the "cold" anomalies, thermometer arrays were read repeatedly during the night mission of May 1968 at two localities in Fish Creek Wash, and thermistor arrays recorded air temperatures continuously for several days in Vallecito Wash. No density stratification of air was detected, and the modern channels were portrayed in both daytime and night-time imagery either not at all or as weak "cold" anomalies.

The slightly low radiance of the modern channels in the Mission 73 imagery may be due to their slightly greater reflectivity (fig. 2). Where the channels were examined with this problem in mind, they are underlain by less vegetative debris. As on the northern half of the Indian Gorge fan (station 3), the slightly lower radiance of the modern channels may be related to their slightly lower concentration of vegetative matter through its effect on 8 to 14 micron emissivity, reflectivity of daytime solar radiation, or both.

Interstitial moisture was found at a depth of 6 to 12 inches beneath the modern channel surfaces, but it did not occur within a foot of the slightly older alluviated surfaces into which the modern channels were incised. Moisture content of the moist zone (2 measurements) was just above 2 percent. Moisture content of the overlying dry sand was less than 0.5 percent. The moisture may be a residuum from previous runoff that has been trapped by surface tension and protected from evaporation by the overlying dry sand. Its effect, if any, on surface temperatures during Mission 73 is unknown.

Figure 17 is a thermal infrared image made shortly after midnight on May 24, 1968, just northeast of the Salton Sea. The bright (highly radiant) area in the northern part of the image is in the headwaters of Salt Creek, a permanent stream draining into the Salton Sea.

Surface materials of both the highly radiant area and the adjacent less radiant terrain include very fine- to fine-grained clayey sand with abundant small mollusk shells--probably deposits of Lake Coahuila, a precursor of the Salton Sea. Springs are abundant in the headwaters of Salt Creek, and large plots of ground are moist. The high night-time radiance occurs where the ground surface is perceptibly moist; the low radiance coincides with dry ground. The region of high radiance includes large areas free of vegetation as well as extensive brushy plots.

More thorough investigation of a somewhat similar occurrence approximately five miles southeast of the Salt Creek headwaters provided documentation of the "warm" anomaly effect of soil moisture in night-time imagery. At this locality (arrow in fig. 17), the San Andreas fault, which coincides with a linear in figure 17, brings fine to coarse grained sand on the east into juxtaposition with red mudstone on the west. The upper surface of the sand, which was visibly moist on May 25, is a thin halite-rich crust. Specific gravity of the sand was approximately 1.4. The moist sand outcrop area coincides approximately with the "warm" anomaly shown by the arrow in figure 17.



Red mudstone west of the fault was mudcracked and visibly dry. Specific gravity was approximately 0.9.

Small dunes of very fine- to medium-grained dry sand overlie the wet sand outcrop. Specific gravity of the dune sand was 1.3. Texturally the dune sand and the underlying sand, except for its halite-rich crust, are relatively similar.

Surface temperature measurements and moisture determinations were made at 5:00 AM on May 26, 1968, as follows:

<u>Material</u>	<u>Moisture content percent</u>	<u>Radiometric temperature °C</u>
Moist sand (crust removed previous day)	8.7	22
Moist sand crust	4.0	20
Partially dry sand crust	1.2	18
Dry dune sand	0.4	17
Crumbly dry mudstone (thin mudcracked crust removed previous day)	3.2 <sup>1/</sup>	16

A direct relationship between soil moisture content and pre-dawn radiance is strongly suggested.

Figure 18 shows near-surface temperatures in the moist sand, dry dune sand, and red mudstone, and temperatures at 5-inch depth in moist sand and dry mudstone. Temperatures were measured by thermistor during a 28-hour period on May 25 and 26, 1968. The near-surface temperature data agree closely with the pre-dawn radiometer measurements of surface temperature. In addition, the near-surface temperatures

---

<sup>1/</sup>No visible moisture; this may represent interlayer water in clay minerals.

illustrate the effect of moisture on thermal inertia at the surface; the wet sand was cooler during the daytime (evaporation may have contributed to this effect) and warmer at night than either the dry sand or dry mudstone. Interstitial water in the moist sand presumably increased its thermal conductivity and heat capacity (i.e., increased its thermal inertia) so that its surface temperature adjusted more slowly to external temperature changes than did surface temperatures of nearby dry sand and mudstone. The night-time temperature difference at 5-inch depth between wet sand and dry mudstone was approximately a third to a fourth of the near-surface difference. This suggests that the near-surface difference was due largely to the lower thermal inertia of the dry mudstone rather than primarily to the introduction of heat in the ground water.

#### Quality of Geologic Information

Figure 19 is a set of infrared images obtained along line 1 from Agua Caliente Springs to the anticline shown in the north-central part of figure 2. Figures 4 to 7, photographs of the axial portion and the western limb of the anticline, show part of the area included in figure 19, and all of the area is shown in figure 2. Comparison of the imagery with the photographs shows that geometric data is of higher quality in the photographs, even in the very small scale (approximately 1:100,000) photograph (fig. 2). This part of the area is underlain by interbedded sandstone and mudstone units that are at best difficult to resolve in the imagery. These units are highly

resolvable in large scale aerial photographs (figs. 4 and 5) and can be at least partially resolved in small scale aerial photographs (fig. 2).

#### Conclusions--Infrared Imagery

Factors thought to influence night-time 8 to 14 micron radiance at site 157 during mission 73 include thermal inertia, reflectivity, and slope angle.

Thermal inertia increases with increasing specific gravity or moisture content. Hence porous weathered gypsum at station 1, which has low specific gravity, has low thermal inertia, and its surface cools rapidly at night. In contrast, at station 4 granite with high specific gravity and moist sand east of the Salton Sea have high thermal inertia, and their surfaces cool less rapidly at night. No satisfactory explanation has been found for the strong "cold" anomalies that represent modern stream channels in the September 1967 imagery. If they represent a soil moisture effect, the effect conflicts with that measured northeast of the Salton Sea and recorded there in the May 1968 (Mission 73) imagery.

Reflectivity may exert significant control on night-time radiance. The alluvial fan at station 3 offers an example of this effect. Currently active anastomosing distributaries have reduced the amount of vegetative matter on the north half of the fan and rendered it more highly reflective than otherwise similar deposits on the adjacent valley floor and on the south half of the fan. The north half of the

fan is presumably less radiant because its higher reflectivity permits less daytime absorption of solar radiation.

Slope angle may strongly influence night-time radiance. Steep slopes (approximately  $30^\circ$ ) near station 2 are highly radiant although they are underlain by deposits similar to those of adjacent gently sloping surfaces ( $10^\circ$  or less) that are characterized by low night-time radiance. Possibly the more nearly horizontal surfaces experience greater night-time radiative loss because they "see" a minimum thickness of atmosphere and a maximum segment of cold sky and, hence, receive minimal radiation from the atmosphere or from other ground surfaces.

The strikingly "cold" anomaly that coincides with the Fish Creek Gypsum outcrop (fig. 13) suggests the possibility of an occurrence of low density surficial material, an inference that could not be made on the basis of aerial photographs alone. In general, however, portrayal of geologic features in the infrared images is disappointing. Geometric information that can be gleaned from the images flown at relatively low altitudes is readily available in 1:100,000 scale aerial photographs (fig. 2). Intertonguing clastic sedimentary units of contrasting lithology are nearly irresolvable in the imagery.

#### MICROWAVE RADIOMETER DATA

Microwave radiometer measurements recorded at 9.2, 15.8, 22.2, and 34.0 GHz were obtained along the two flight lines from an altitude of several thousand feet in the early afternoon of May 21, 1968.

Curves plotted for the 15.8, 22.2, and 34.0 GHZ frequencies oscillate with low amplitude largely between 275 and 295°K. (fig. 20). They show no distinctive peaks or troughs that can be related to geologic features. Locations of geographic features noted on figure 20 were estimated on the basis of time elapsed during the flight.

The curve plotted for the 9.2 GHZ frequency is characterized by high amplitude oscillations that range from 0 to nearly 300°K. On line 1, from Agua Caliente Springs to Lower Borrego Valley immediately east of the Fish Creek Mountains, a broad trough coincides roughly with the belt of alternating mudstone and sandstone that crops out between Agua Caliente Springs and Split Mountain. Figure 14 shows the major geologic features of the Split Mountain-Fish Creek Mountains area. No distinctive troughs or peaks occur at or east of Split Mountain. Line 2 was flown from Indian Valley across the Fish Creek Mountains (fig. 2) to the Salton Sea. Through the granite of Indian Gorge and the interbedded sandstone and mudstone between Vallecito Wash and Split Mountain, the 9.2 GHZ curve hovers mainly near 275°K and is largely featureless. A prominent trough coincides approximately with Split Mountain, and a second occurs in Lower Borrego Valley just east of the Fish Creek Mountains. The inconsistent relationship between geologic features and 9.2 GHZ data on the two flight lines (table 1) suggests that the microwave data bear no simple relationship to major geologic features.

Table 1.--Summary of broad 9.2 GHZ microwave data and major geologic features .

Geologic feature	Microwave data	
	Line 1	Line 2
Granite of Indian Gorge	-----	flat curve
Interbedded sandstone and mudstone	broad trough	flat curve
Split Mountain	featureless	steep trough
Fish Creek Mountains	featureless	featureless
Lower Borrego Valley	featureless	steep trough at west edge

#### REFERENCES

- Dibblee, T. W., Jr., 1954, Geology of the Imperial Valley region, California, in Geology of southern California: Calif. Div. Mines Bull. 170, Ch. 2, p. 21-28, pl. 2.
- Pease, R. W., and Bowden, L. W., 1968, Making color infrared film a more effective high altitude sensor: U.S. Geol. Survey Tech. Letter NASA-117.
- Sabins, F. F., Jr., 1967, Infrared imagery and geologic aspects: Photogrammetric Engineering, v. 33, no. 7, p. 743-750.
- Wallace, R. E., and Moxham, R. M., 1966, Use of infrared imagery in study of the San Andreas fault system, California: U.S. Geol. Survey Tech. Letter NASA-42; 1967, Use of infrared imagery in study of the San Andreas fault system, California, in Geological Survey Research 1967: U.S. Geol. Survey Prof. Paper 575-D, p. D147-D156; abs. in Symposium Remote Sensing of Environment, 4th, Michigan Univ., Ann Arbor, Infrared Physics Lab., Abstracts, p. 24.

Wolfe, E. W., 1968, Geologic evaluation of thermal infrared imagery,  
Caliente and Temblor Ranges, southern California: U.S. Geol.  
Survey Tech. Letter NASA-113.

Woodard, G. D., 1963, The Cenozoic stratigraphy of the western Colorado  
Desert, San Diego and Imperial Counties, southern California:  
Unpublished doctoral dissertation, Univ. of Calif., Berkeley,  
165 pp.

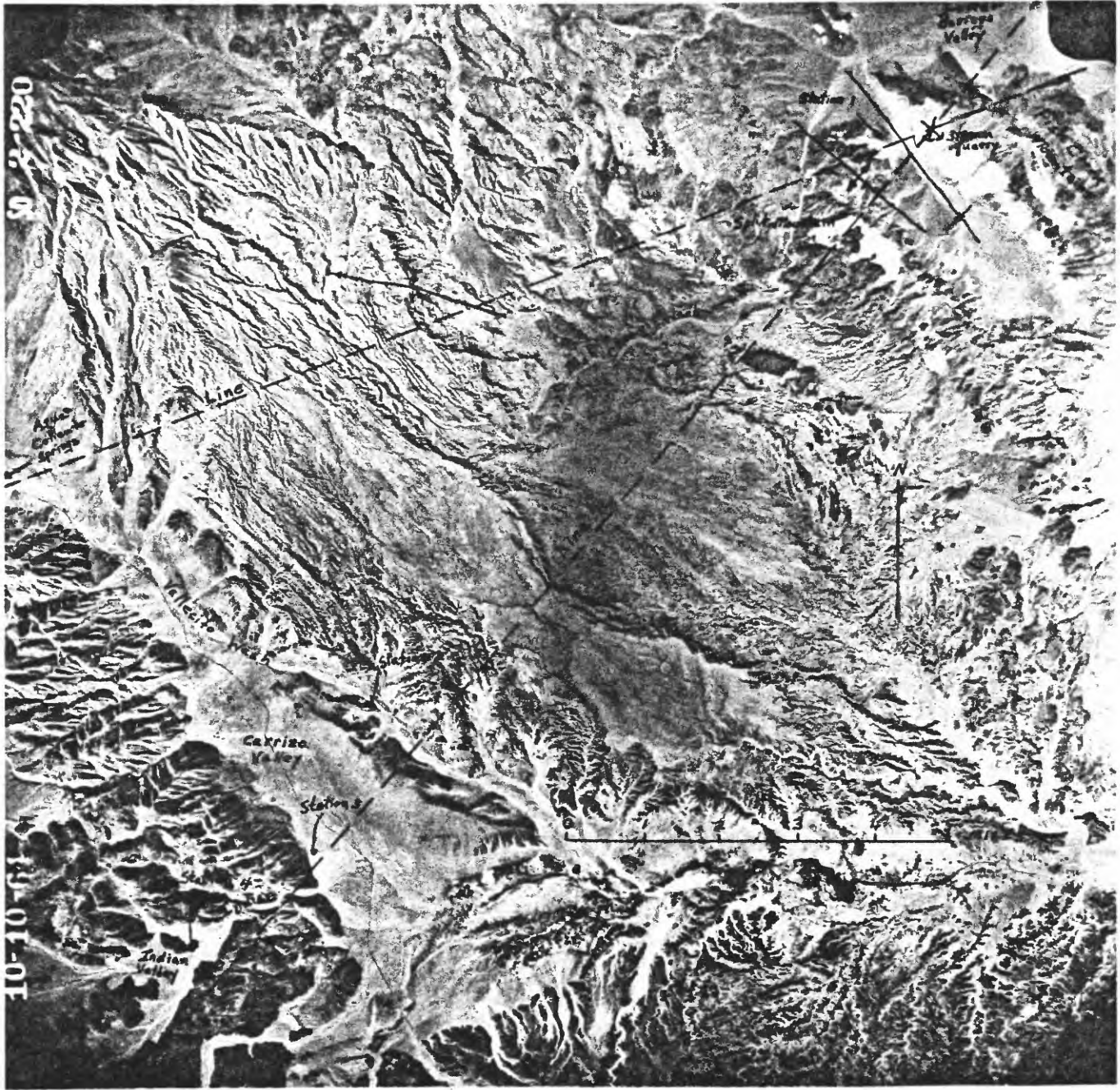
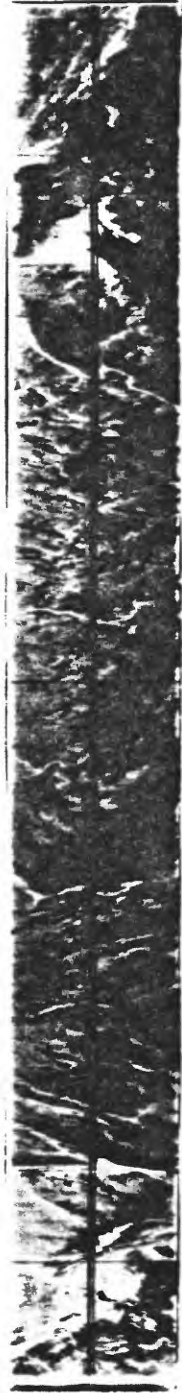


Figure 2.--High-altitude aerial photograph of site 157.





Fish Creek  
Mountains

Split  
Mountain

Aqua  
Caliente  
Springs

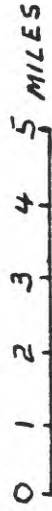


Figure 3.--AN/AAS-5 ultraviolet scan imagery, site 157, line 1.

Figure 4.--Black and white aerial photograph taken over anticline crest near center of line 1, site 157. Photographed area is approximately  $1\frac{1}{2}$  miles wide. Clock on southwest edge of photograph.

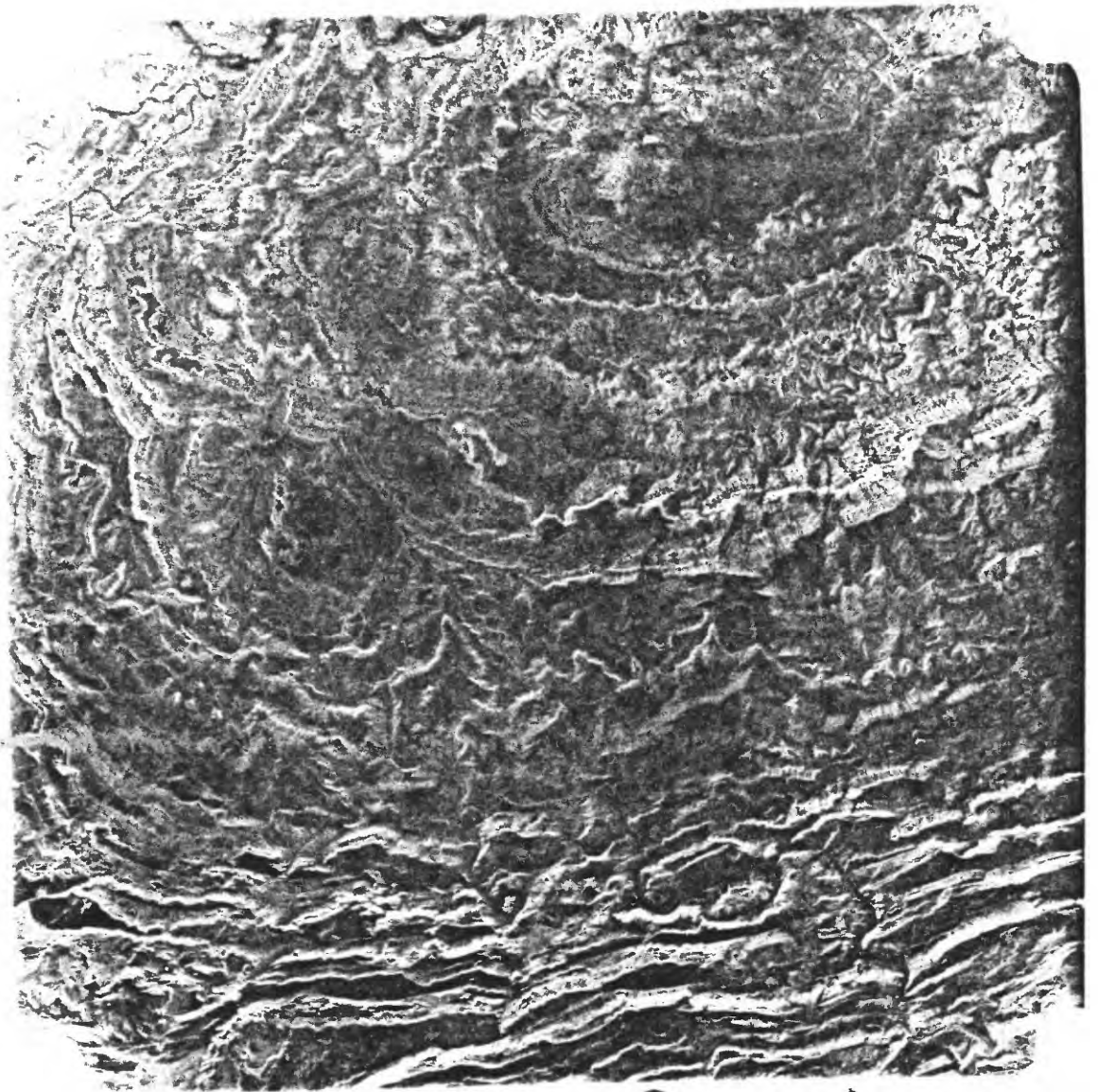


Figure 4.

Figure 5.--Aero-Ektachrome Infrared (8443) aerial photograph taken over anticline crest near center of line 1, site 157. Photographed area is approximately 1½ miles wide. Clock on southwest edge of photograph.

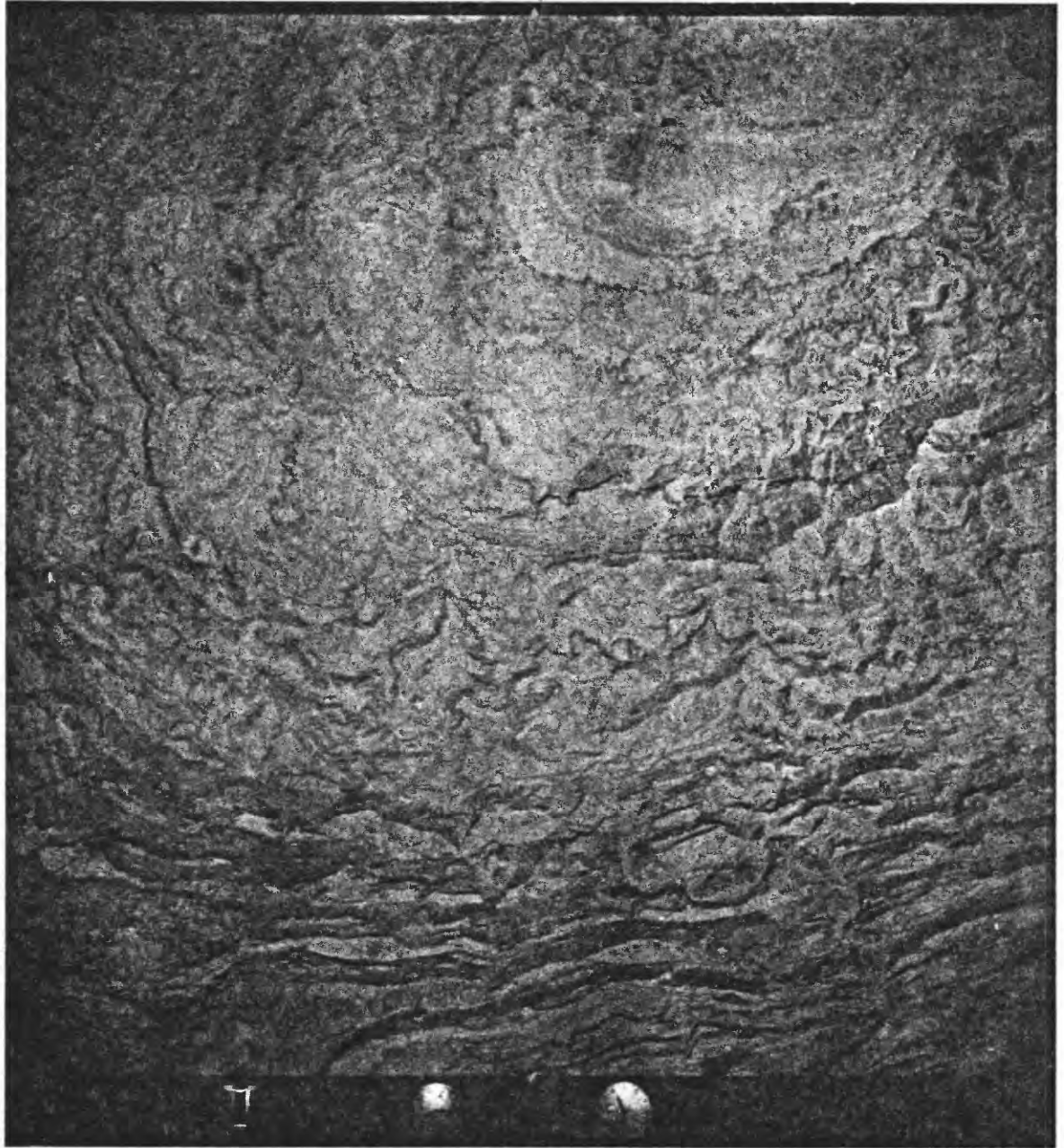


Figure 5

Figure 6.--Kodachrome taken from 15,000 feet over axial portion of anticline near center of line 1, site 157.

Figure 7.--Kodachrome taken from a ridge top in the axial portion of the anticline near the center of line 1.

Figure 8.--Kodachrome showing pink sandstone and dark gray sandy mudstone exposed on southwest flank of anticline near center of line 1, site 157. Vallecito Mountains in background.

Figure 9.--False color photograph (Ektachrome Infrared 8443 + Wratten 15 filter) of same scene as figure 8.

Figure 10.--False color photograph (Ektachrome Infrared 8443 + Wratten 15 and CC30M filters) of same scene as figure 8.

Figure 11.--False color photograph (Ektachrome Infrared 8443 + Wratten 15 and CC30B filters) of same scene as figure 8.

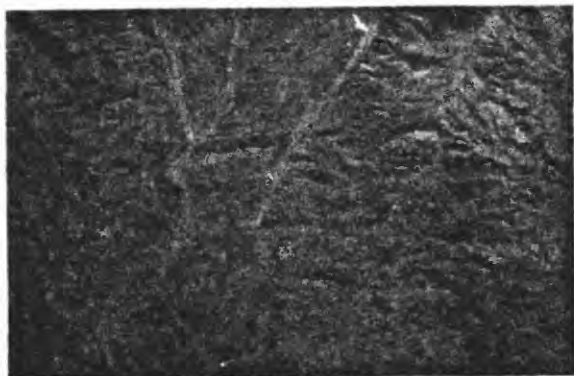


Figure 6.

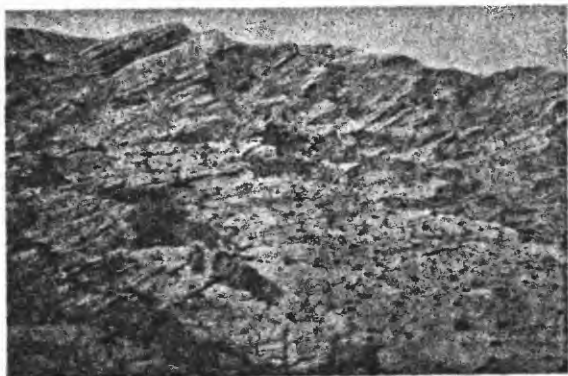


Figure 7.



Figure 8.



Figure 9.

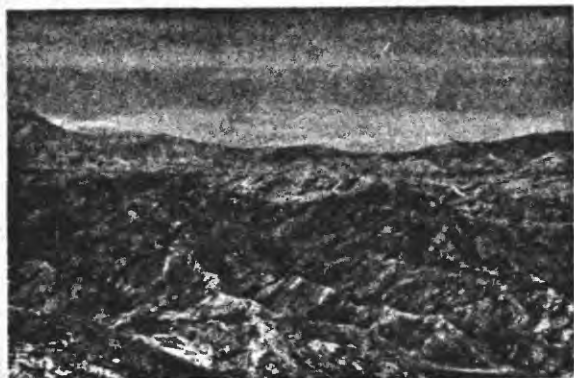


Figure 10.

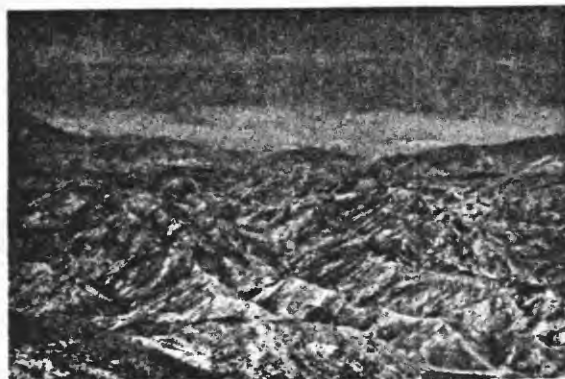


Figure 11.

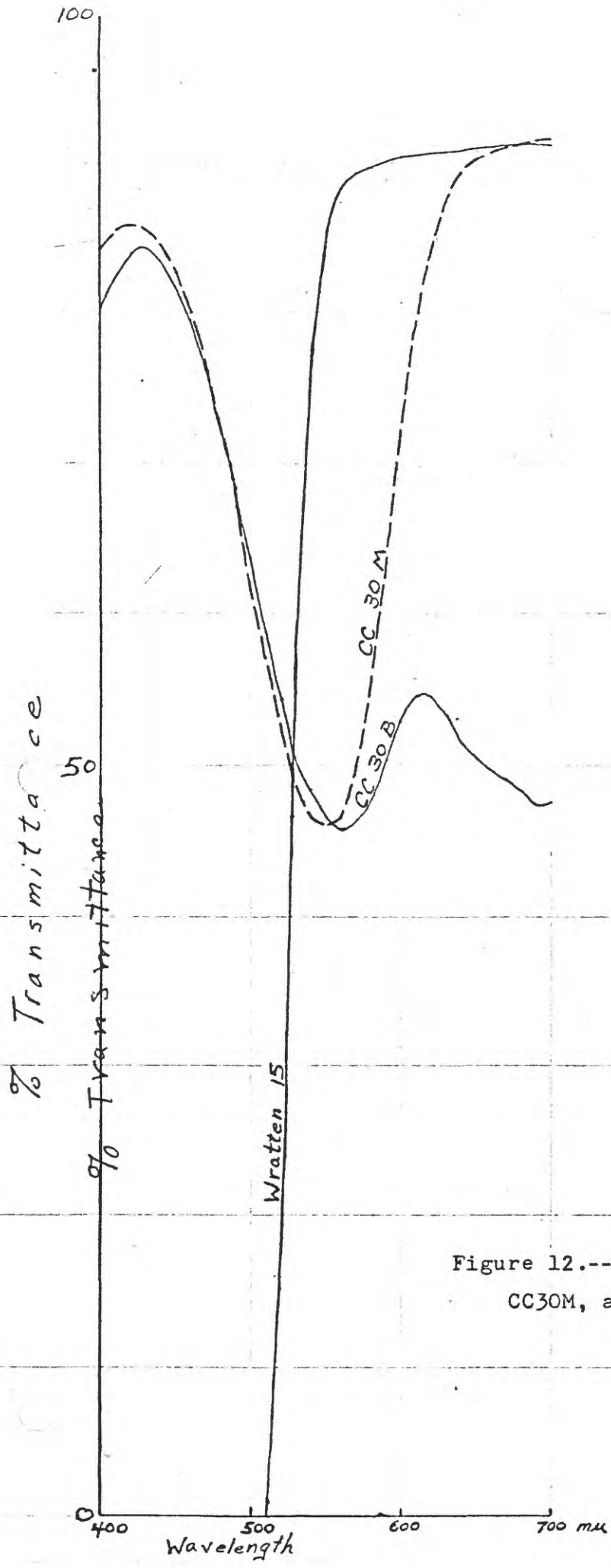
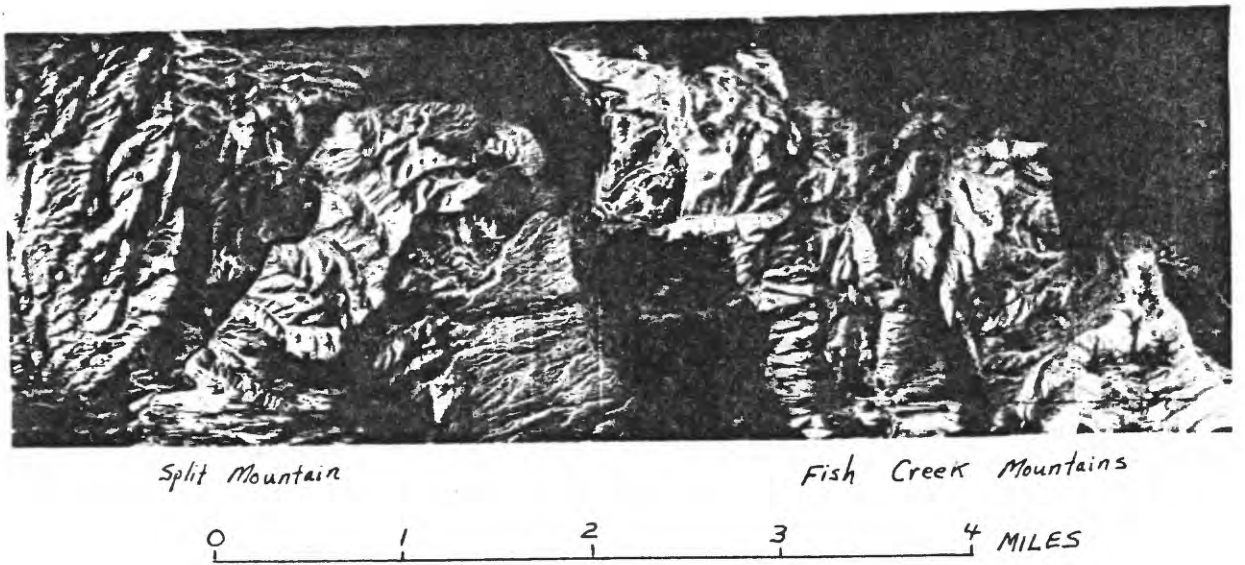
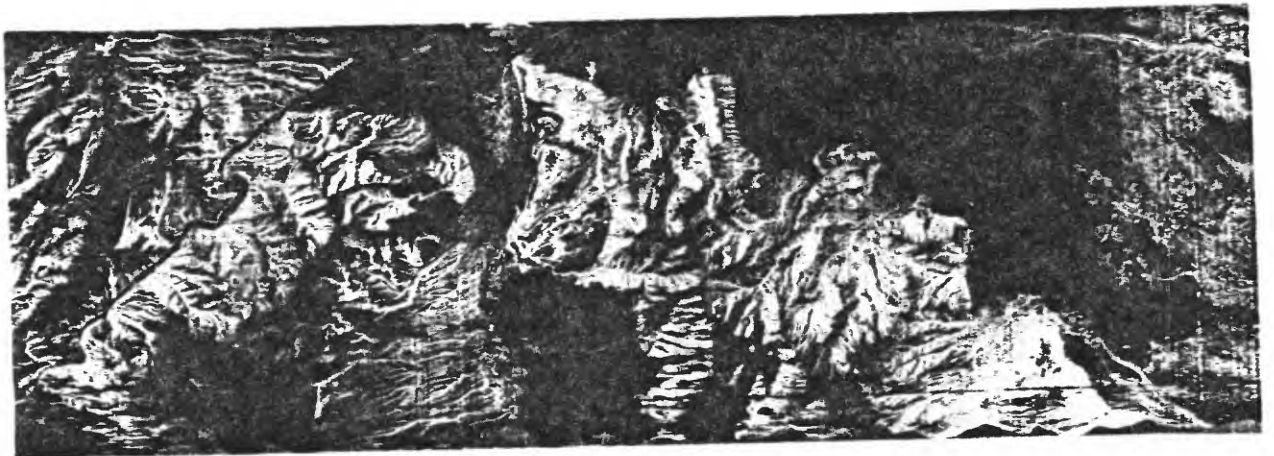


Figure 12.--Transmission curves for Wratten 15, CC30M, and CC30B filters.





a. pre-sunset (1934)

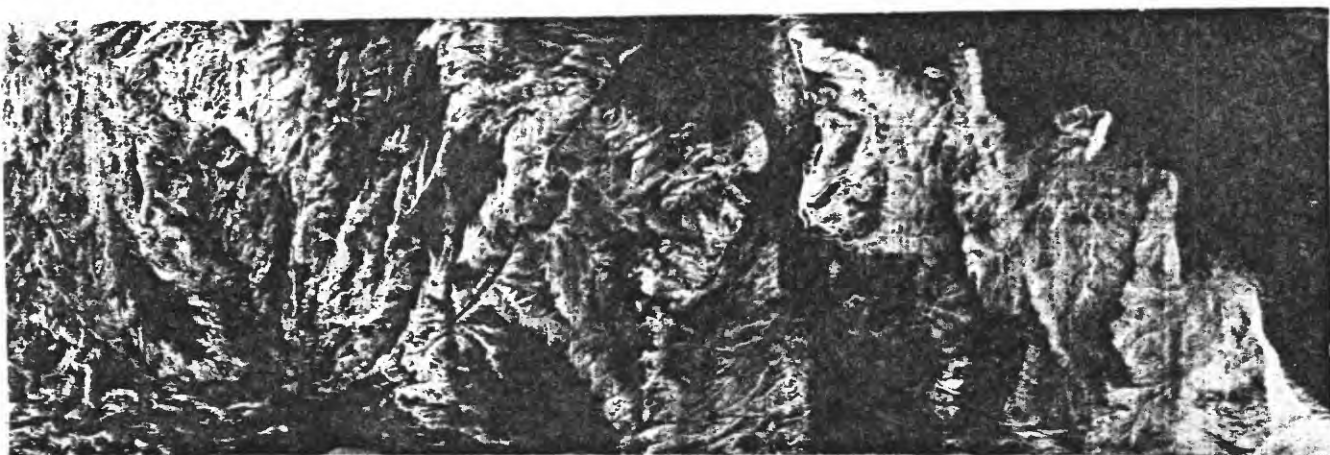


b. post-sunset (2040)

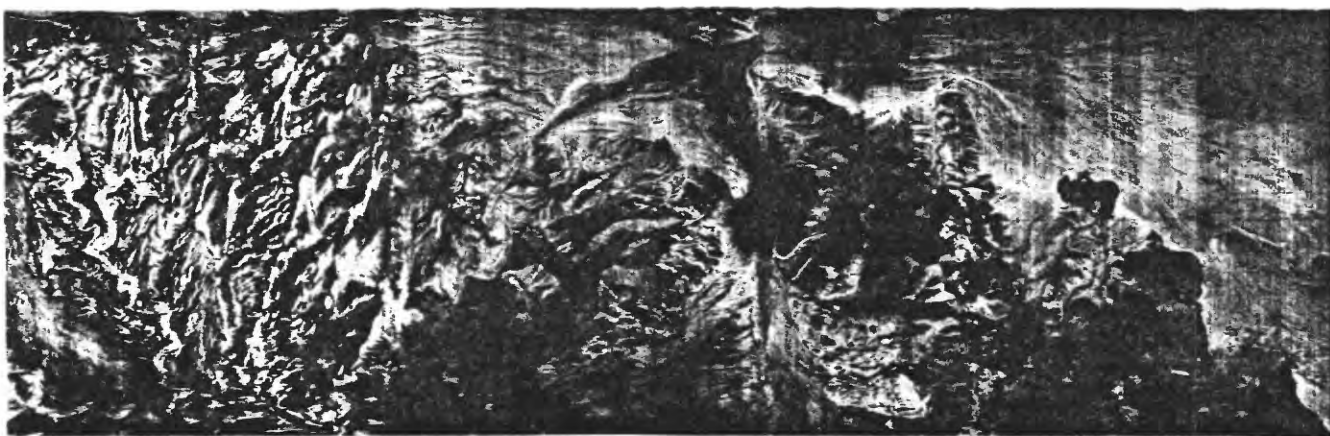
Figure 13.--Thermal infrared images of the eastern part of line 1, including station 1.



*c. pre-sunrise (0515)*

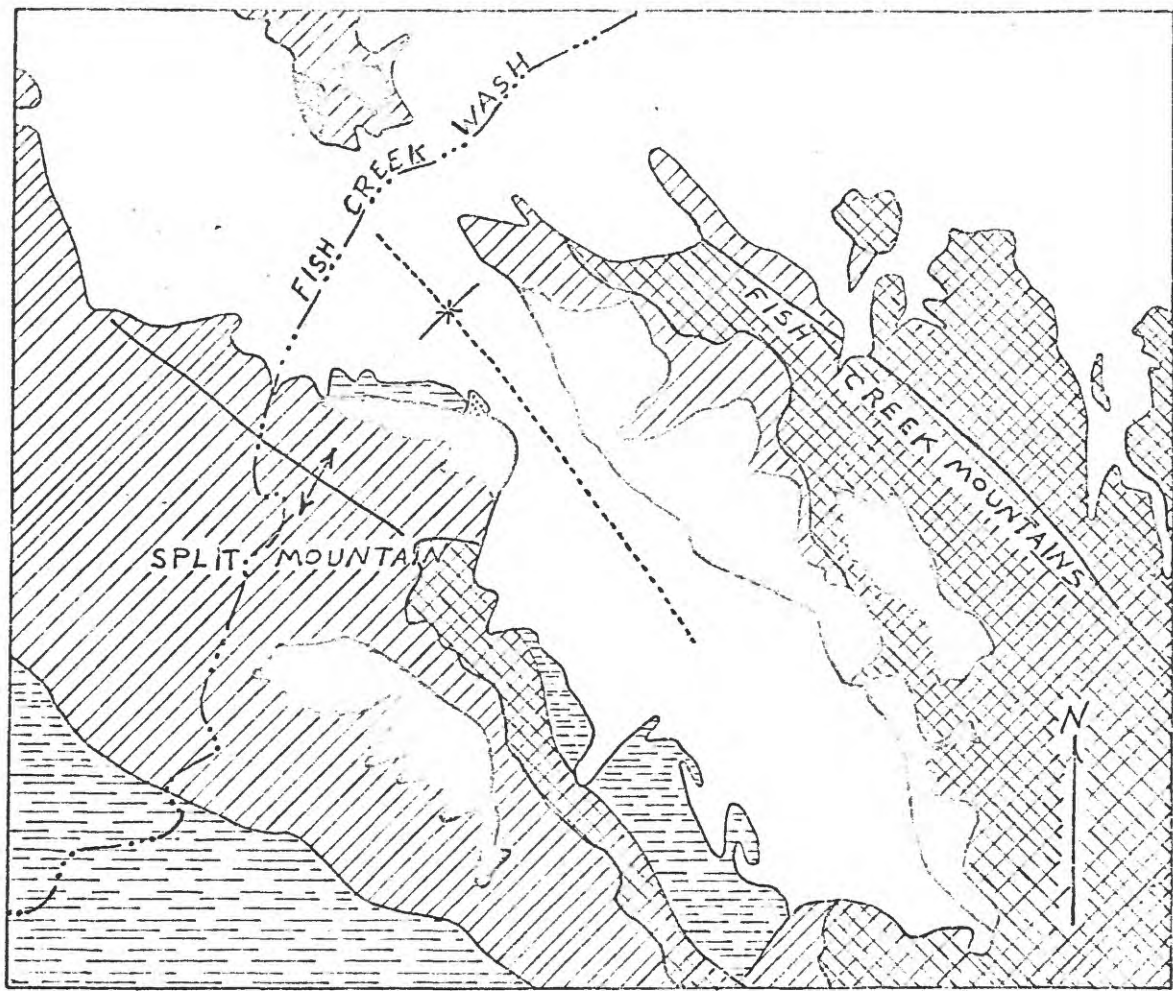


*d. post-sunrise (0615)*



*e. Midday*

Figure 13 cont.



0 1 2 3 4 MILES

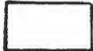
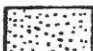




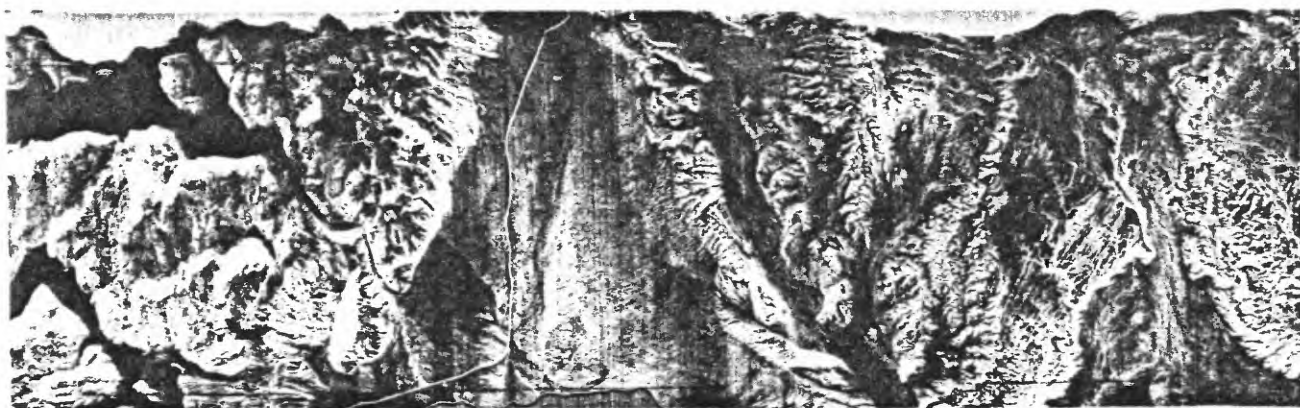
-  Younger alluvium; sand and gravel in modern washes
-  Older alluvium; sand, gravel, and cobbles of granitic debris
-  Imperial Formation; mudstone, some sandstone
-  Fish Creek Gypsum
-  Split Mountain Formation; conglomerate, sandstone, minor mudstone
-  Pre-Tertiary crystalline rocks

Figure 14.--Generalized geologic map of the Split Mountain-northwestern Fish Creek Mountains area (after unpublished geologic maps by Dibblee).



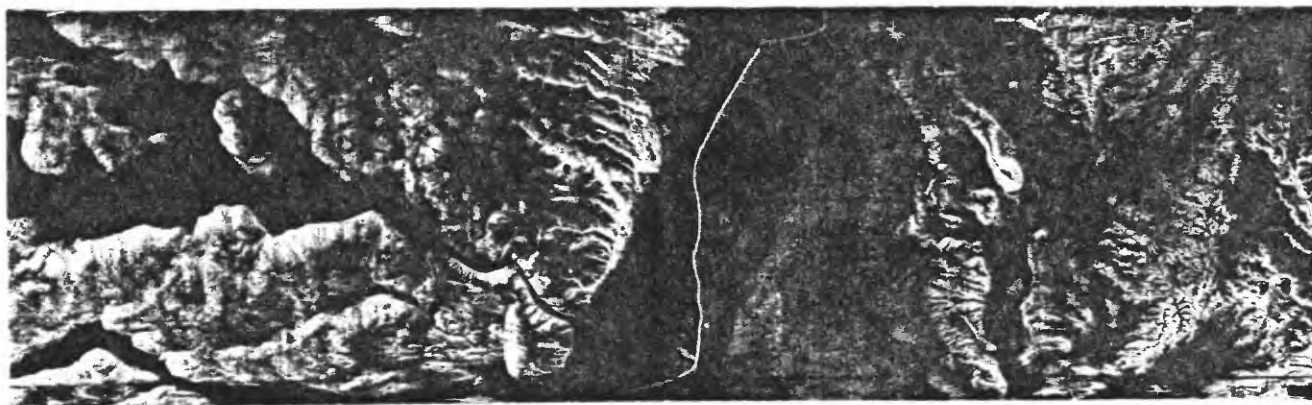
Figure 15.--Station 2. Cliff of barely consolidated pebbly sandstone overlain by bouldery gravel deposit. Bouldery colluvium discontinuously mantles sandstone outcrop. Truck stands on modern channel floor at base of cliff.



Indian Valley      Indian Gorge      Carrizo Valley      Vallecito Wash

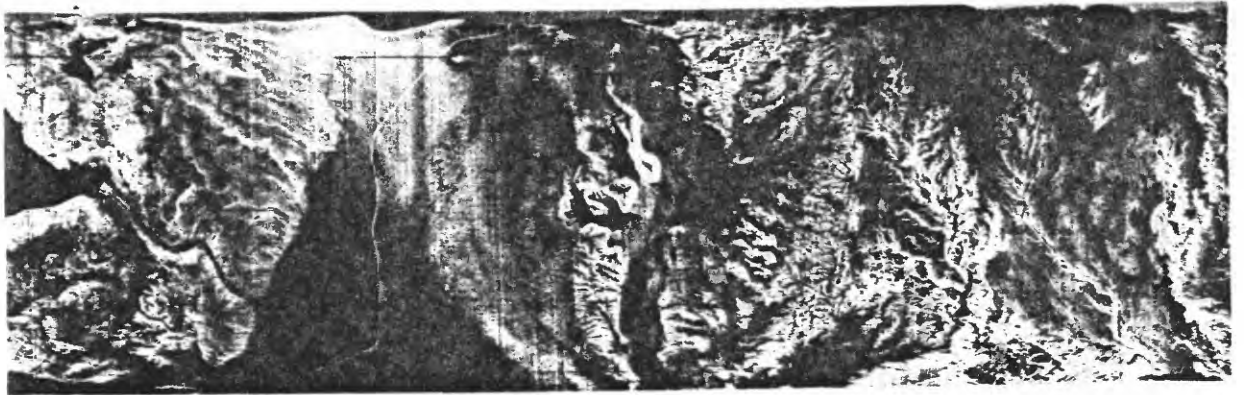
0      1      2      3      4 MILES

a. pre-sunset (1922)

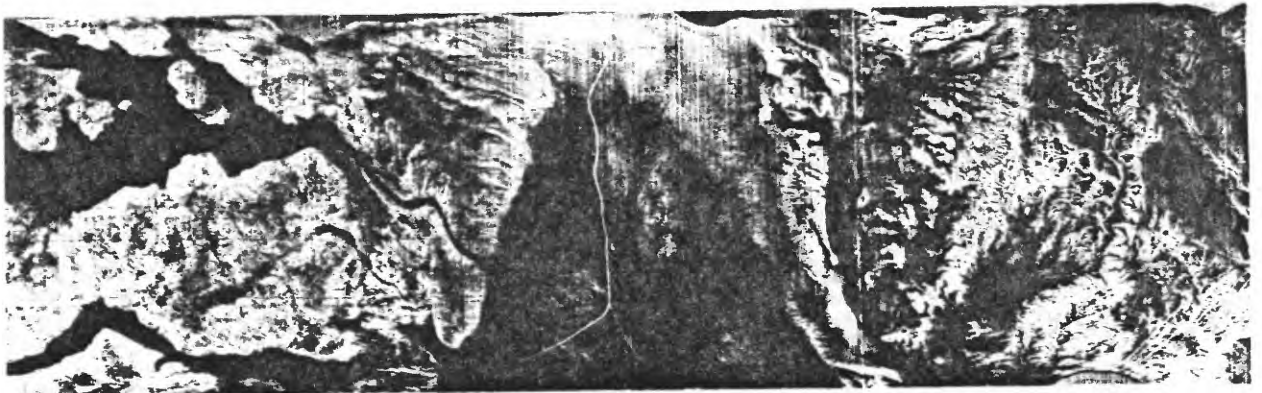


b. post-sunset (2029)

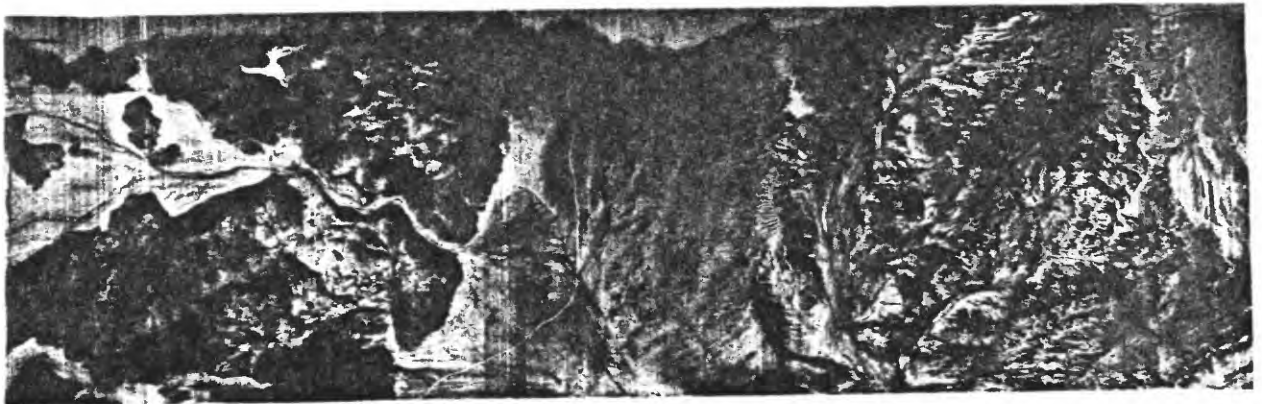
Figure 16.--Thermal infrared images of the southwestern part of line 2. Includes stations 2, 3, and 4.



c pre-sunrise (0504)



d post-sunrise (0605)



e midday (1325)



Figure 17.--Thermal infrared image made shortly after midnight on May 24, 1968, northeast of the Salton Sea in the Salt Creek area. See figure 1 for location.

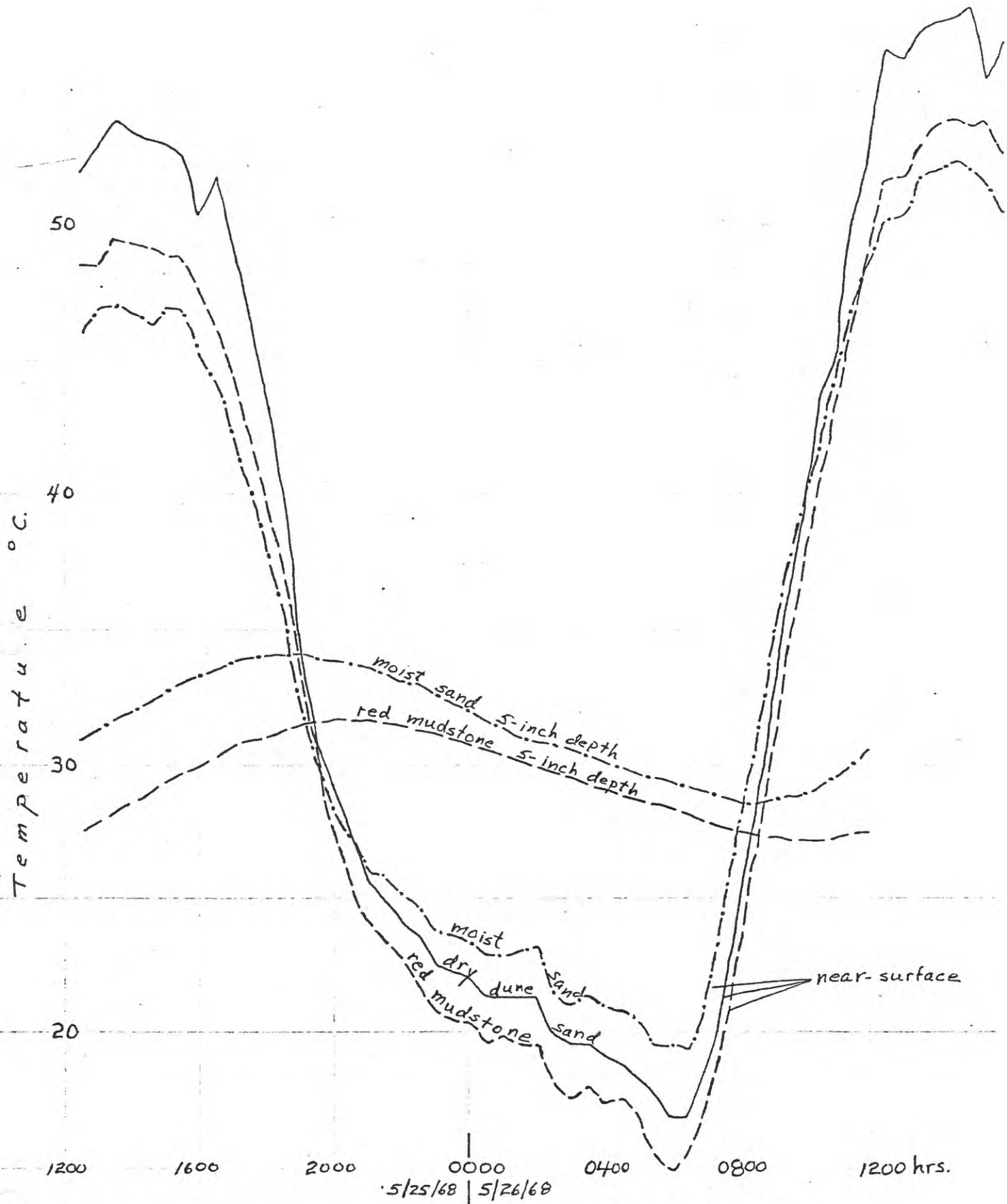


Figure 18.-- Thermistor temperatures of surficial materials near San Andreas fault on northeast side of Salton Sea.





Aqua  
Caliente  
Springs

a. pre-sunset (1929)

0 1 2 3 4 MILES



b. post-sunset (2035)

Figure 19.--Thermal infrared images of the western part of line 1.



*c. pre-sunrise (0510)*



*d. post-sunrise (0610)*



*e. midday (1310)*

MISSION 73, FLIGHT 1, LINE 1

Agua Caliente Springs

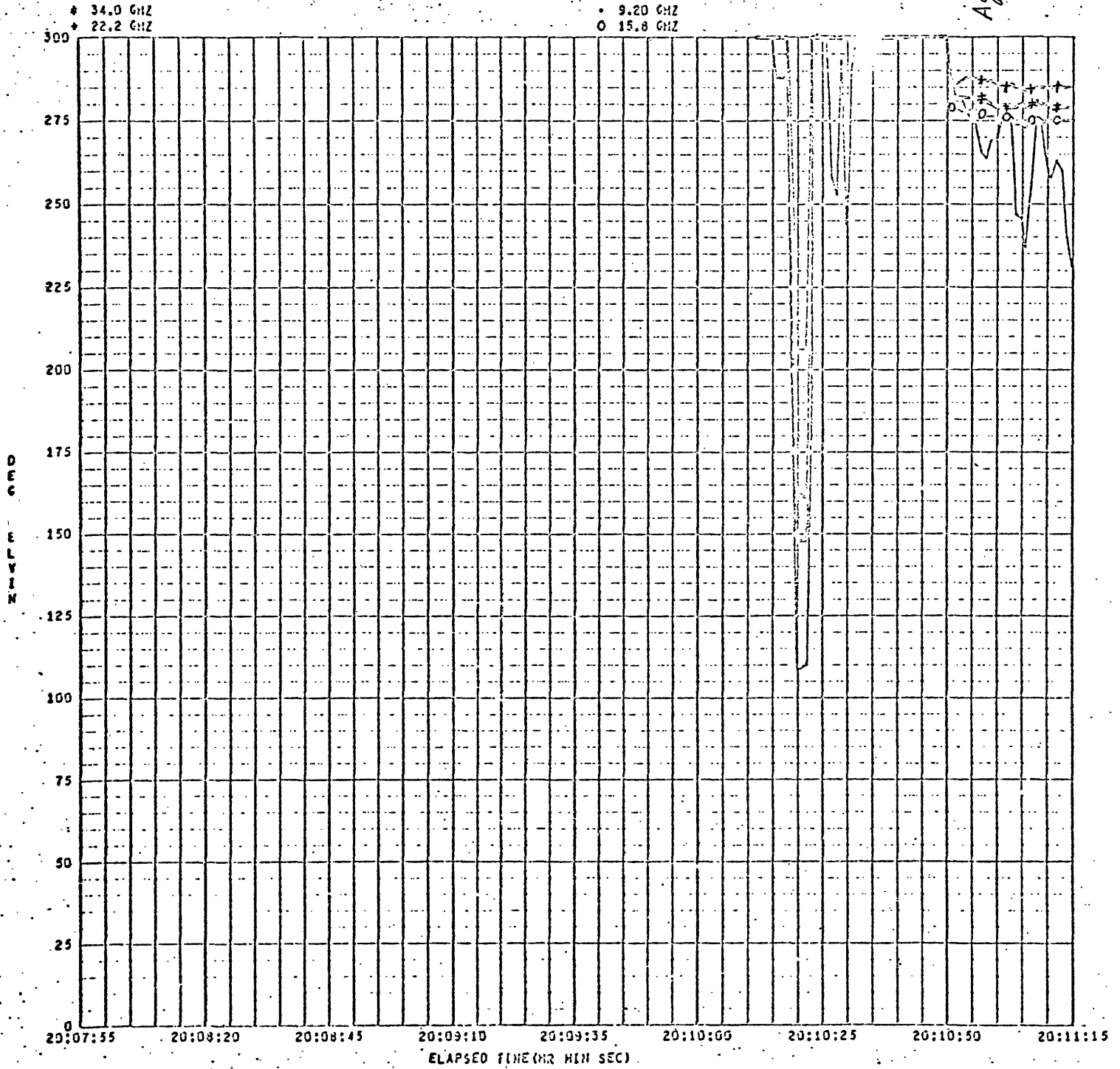


Figure 20--Microwave data, Mission 73, site 157.

MISSION 73, FLIGHT 1, LINE 1

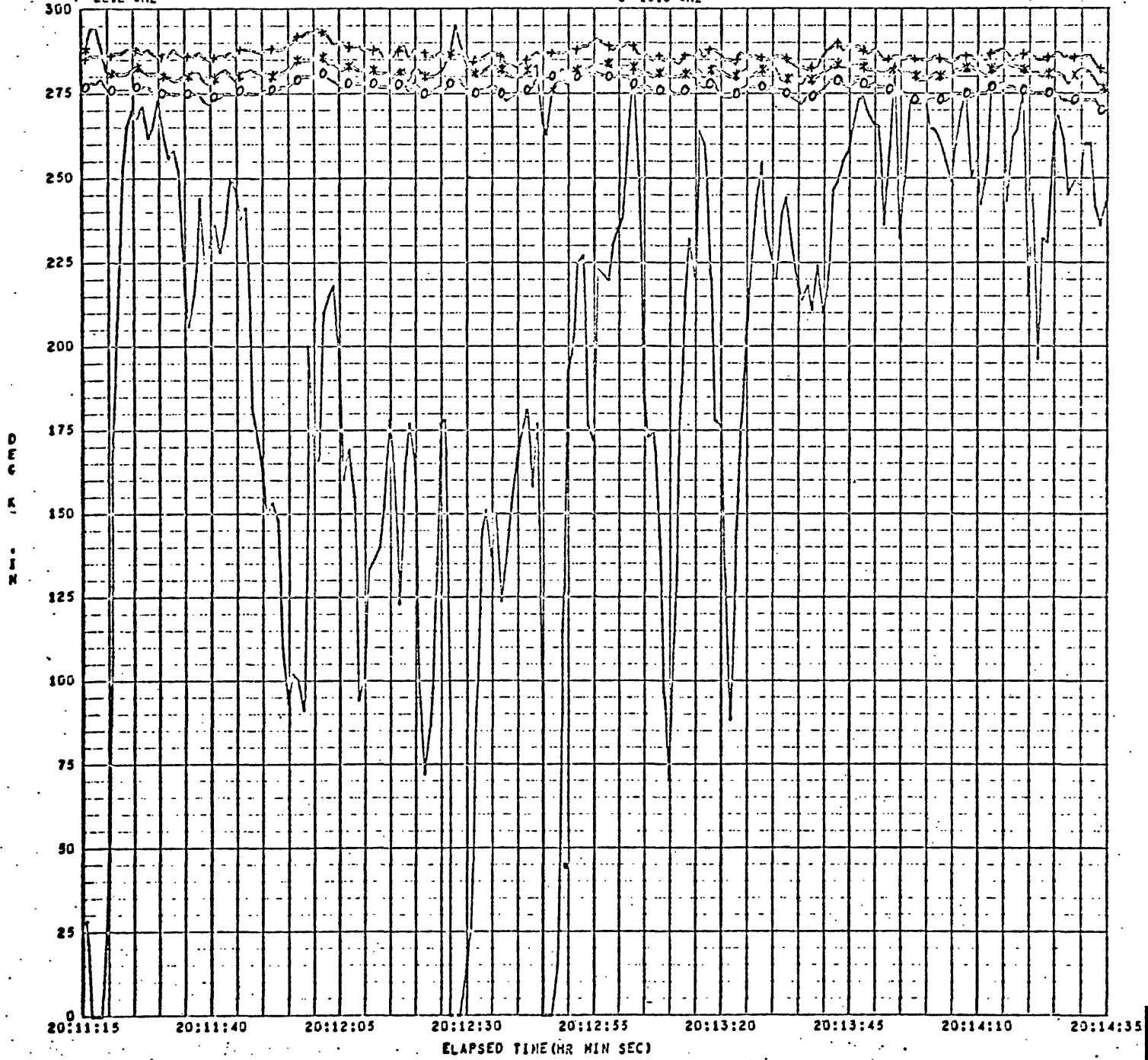
*Anticline crest*

*Split Mountain*

*Fish Creek Mountains*

\* 34.0 GHZ  
+ 22.2 GHZ

• 9.20 GHZ  
○ 15.8 GHZ



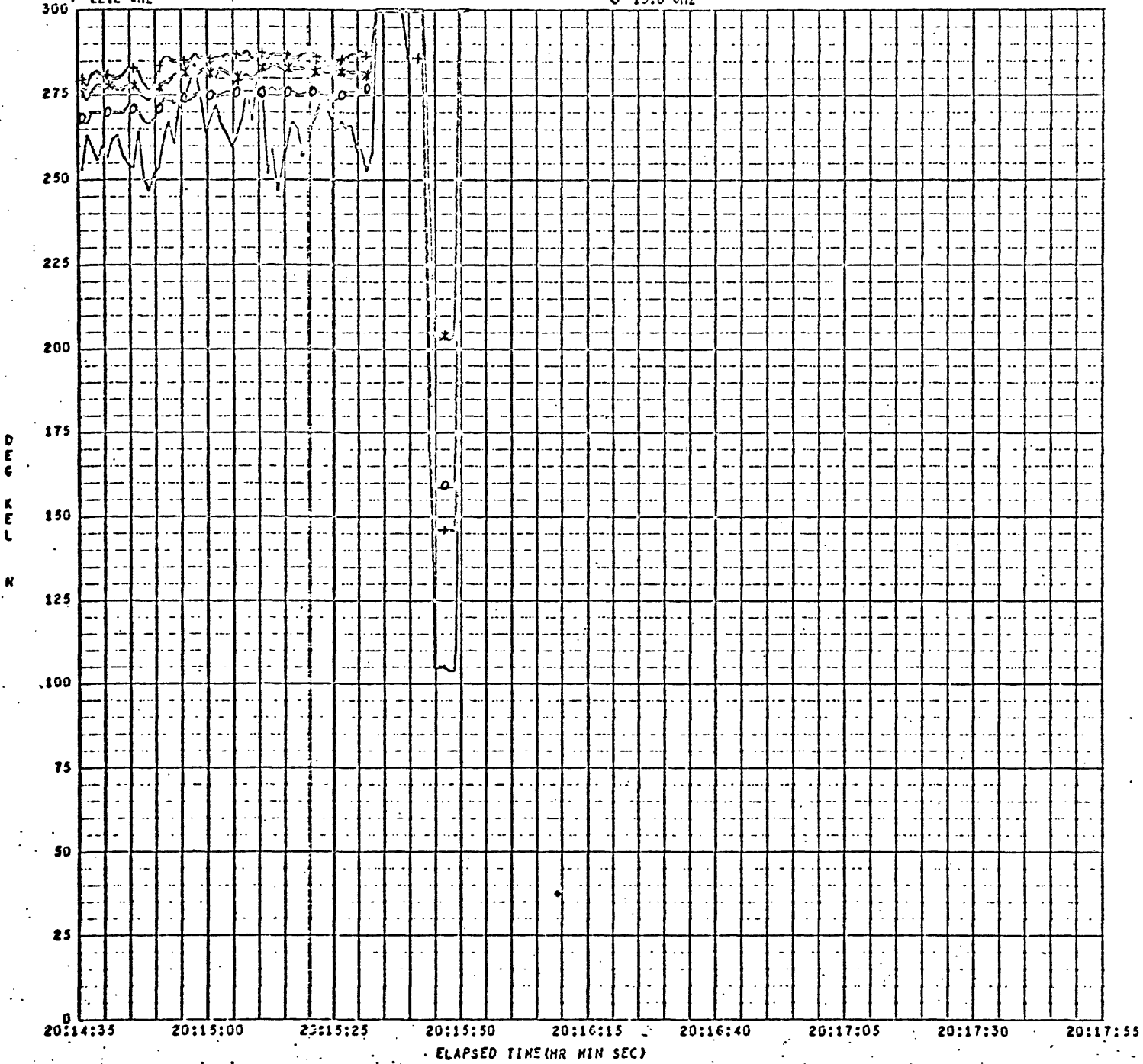
Fish Creek  
Mountains

Lower Borrego  
Valley

MISSION 73, FLIGHT 1, Line 1

\* 34.0 GHZ  
♦ 22.2 GHZ

• 9.20 GHZ  
O 15.8 GHZ



Indian Valley

Indian Gorge

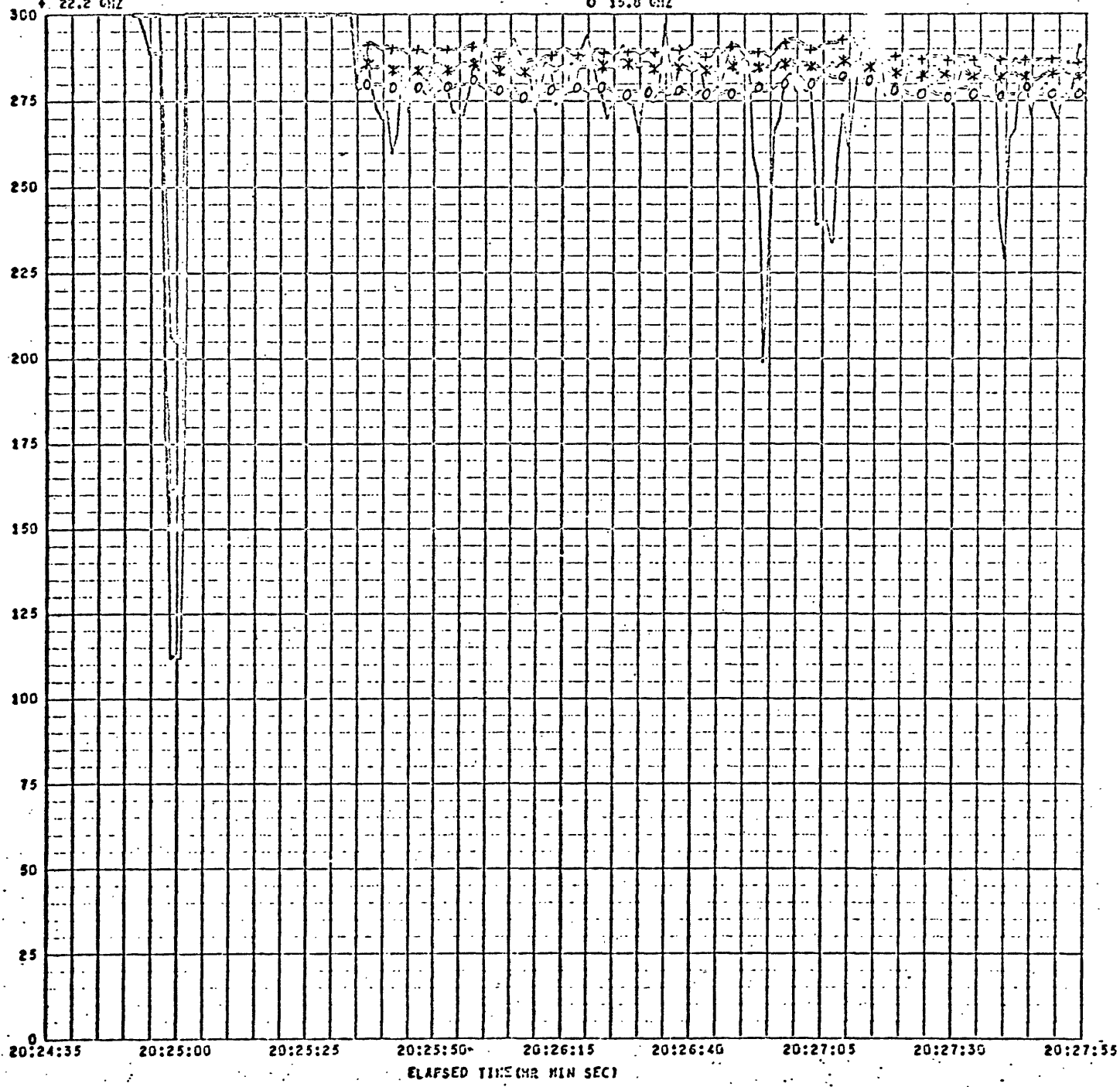
Vallecito Wash

MISSION 73, FLIGHT 1, LINE 2

\* 34.0 GHz  
+ 22.2 GHz

• 9.20 GHz  
o 15.8 GHz

2m. 97.6MD



Split Mountain

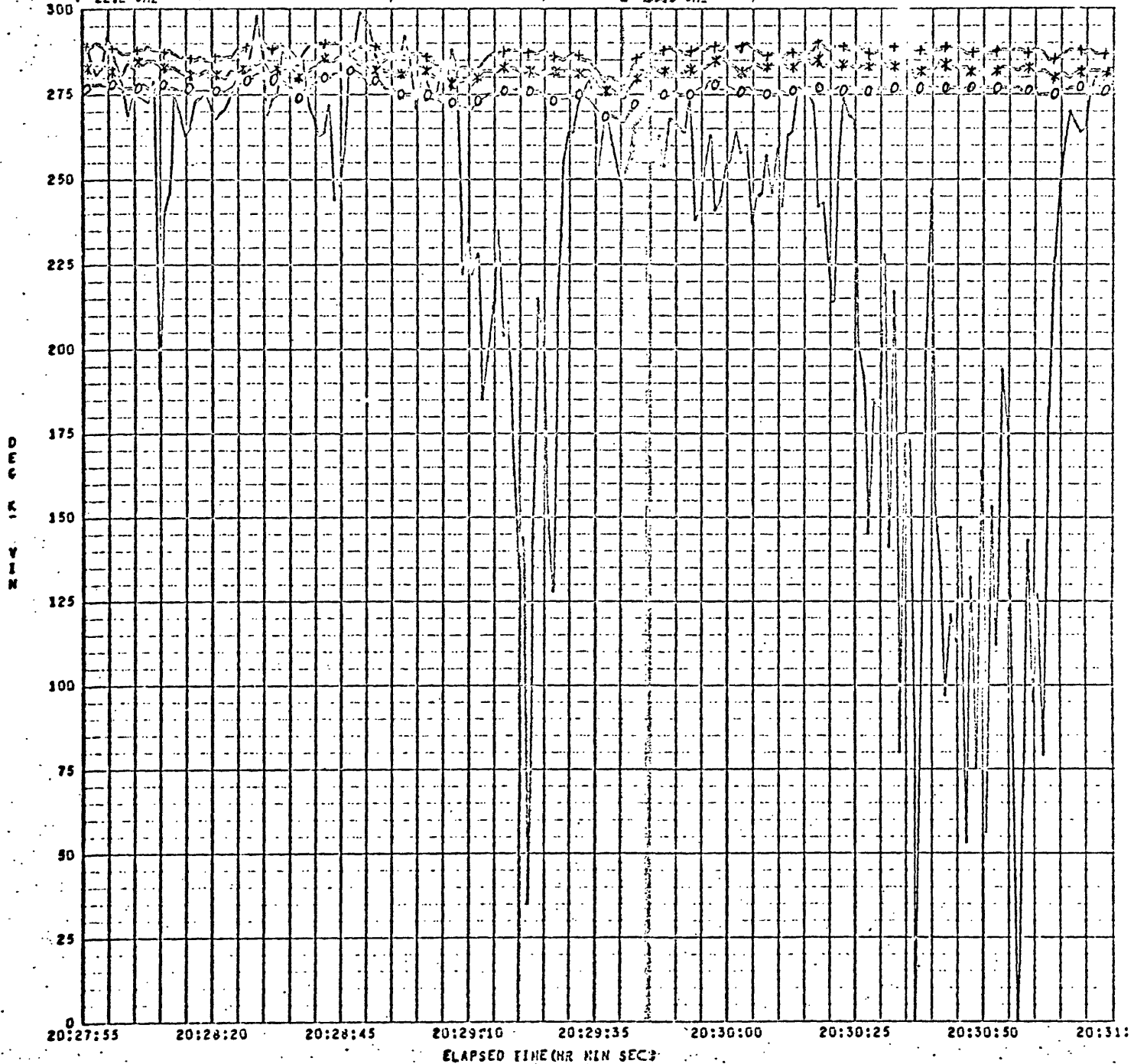
Fish Creek  
Mountains

Lower Borrego  
Valley

MISSION 73, FLIGHT 1, LINE 2

\* 34.0 GHz  
• 22.2 GHz

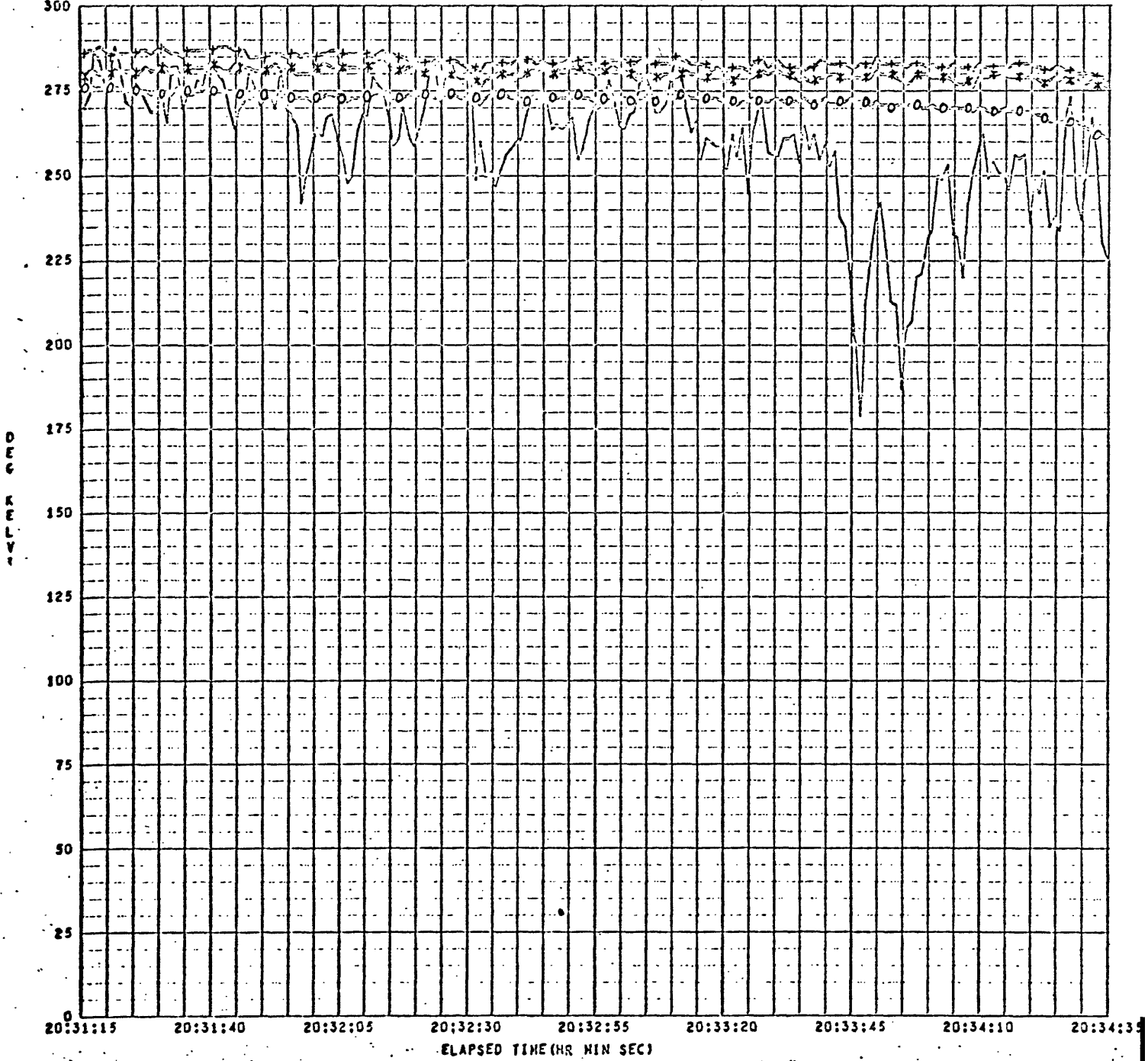
○ 25.8 GHz  
○ 25.8 GHz



MISSION 73, FLIGHT 1, Line 2

\* 34.0 CHZ  
+ 22.2 CHZ

• 9.20 CHZ  
○ 15.8 CHZ





Saltion Sea

MISSION 73, FLIGHT 1, LINE 2

\* 34.0 GHZ  
+ 22.2 GHZ

• 9.20 GHZ  
o 15.8 GHZ

